Strong surface winds in Storm Eunice. Part 1: storm overview and indications of sting-jet activity from observations and model data

Volonté, A. ORCID: https://orcid.org/0000-0003-0278-952X, Gray, S. L. ORCID: https://orcid.org/0000-0001-8658-362X, Clark, P. A. ORCID: https://orcid.org/0000-0003-1001-9226, Martínez-Alvarado, O. ORCID: https://orcid.org/0000-0002-5285-0379 and Ackerley, D. (2024) Strong surface winds in Storm Eunice. Part 1: storm overview and indications of sting-jet activity from observations and model data. Weather, 79 (2). pp. 40-45. ISSN 1477-8696 doi: 10.1002/wea.4402 Available at https://centaur.reading.ac.uk/111437/

Strong surface winds in Storm *Eunice*. Part 1: storm overview and indications of sting jet activity from observations and model data

Ambrogio Volonté[1,*], Suzanne L. Gray[1], Peter A. Clark[1], Oscar Martínez-Alvarado[1,2] and Duncan Ackerley[3]

[1]*Department of Meteorology, University of Reading, UK*
[2]*National Centre for Atmospheric Science, University of Reading, UK*
[3]*Met Office, Exeter, UK*

Introduction

Storm *Eunice* was the second of three named storms to affect the United Kingdom (UK) within a week during February 2022. Figure 1a shows the publicly issued information by the Met Office National Severe Weather Warning Service (NSWWS[1]) for *Eunice* with two red warning regions for wind over southern England, including London, together with an amber wind warning covering most of England and Wales.

The NSWWS was instigated in 1988 in the aftermath of the 'Great Storm' of 15/16 October 1987 that devastated southeast England (Burt and Mansfield, 1988); since early 2011 warnings have been based on an 'impact matrix' considering both likelihood and impact, with red meaning there is a high likelihood of a high impact. This was the second red warning for wind issued in the 2021/2022 season, but particularly notable as the first time a red wind warning had been issued for southeast England since the service began.

Although *Eunice* brought rainfall and snowfall, the primary hazard was wind. Though not as devastating as the Great Storm (not least because of the actions taken as a result of the warning), *Eunice* still led to severe weather impacts in the UK and Ireland, including four fatalities, loss of power to over a million homes, thousands of felled trees, damage to buildings (including the roof of the O2 Arena in London), transport disruption and the closure of schools and businesses. An account of the UK impacts and observations for all three named storms, together with the historical context of Storm *Eunice*, is given in a Met Office report (Kendon, 2022). Storm *Eunice* (subsequently under the name *Zeynep*) went on to cause severe disruption in northern Belgium, the Netherlands, the northern half of Germany and the southwestern Baltic Sea region. In these later stages over the continent, the main impact arose from an intense cold front bringing convection and high winds (Mühr *et al.*, 2022). Here we summarise key meteorological aspects of the storm in its relatively early stages, focusing on the structure of the storm and evidence for the presence of a 'sting jet'.

Storm *Eunice* tracked rapidly across the North Atlantic from its initiation. At 0600 UTC on 16 February, *Eunice* existed as a weak system at about 40°N, 50°W. It deepened explosively in the 24h prior to 0000 UTC 18 February (and in particular in the previous 12h, when the central mean sea-level pressure dropped by 27hPa), at which time it was located to the southwest of Ireland with a central pressure of 975hPa. The central pressure of 975hPa remained largely unchanged as *Eunice* tracked across the southern UK and Ireland over the next 12h. Figure 1b shows the analysis chart at 0600 UTC on 18 February when the centre of the storm was located just south of Ireland. The roof of the O2 Arena was damaged as the storm tracked across London at around 1200 UTC.

While strong surface winds in extratropical cyclones are commonly associated with the synoptic-scale warm and cold conveyor belts, an additional airstream, the sting jet (SJ), can be found in some cyclones that follow the Shapiro–Keyser cyclone model. A more detailed description of these airstreams is given in part 2 (Volonté *et al.*, 2023) of this study. The SJ was first proposed by Browning (2004) as a result of analysis of the spatial distribution of extreme gusts in the 'Great Storm'. The most damaging surface winds occurred at the tip of an airstream, dubbed the SJ, that descended from the tip of the cloud head into the widening frontal-fracture region, behind the primary cold front and ahead of the bent-back front and cloud head. Since the pioneering studies of the Great Storm, SJs have been analysed in several other storms and are suspected to be a fairly common feature of intense Shapiro–Keyser extratropical cyclones (Hart *et al.*, 2017). For a general overview of the

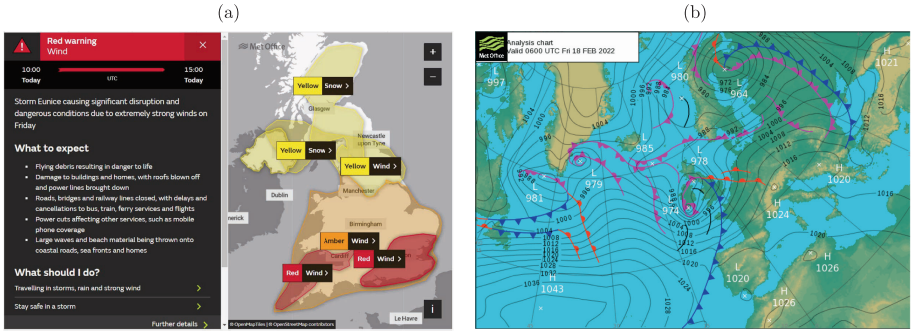

Figure 1. (a) Met Office National Severe Weather Warning Service (NSWWS) red weather warnings issued for 18 February 2022 (Crown copyright). (b) Met Office analysis chart at 0600 UTC. (© Crown copyright.)

[1]https://www.metoffice.gov.uk/weather/guides/severe-weather-advice.

SJ, see Schultz and Browning (2017), while Clark and Gray (2018) provide an in-depth review.

This article, the first of a two-part study on Storm *Eunice*, takes advantage of observations from weather stations and satellite imagery to explore *Eunice*'s structure, assessing whether it has the Shapiro–Keyser structure necessary for a SJ to form and, if so, investigating any evidence of SJ activity. Operational Met Office forecast model data are used to highlight the evolution of Storm *Eunice*'s forecasts in the run up to its passage over the UK, focusing on overall storm structure and smaller-scale peak-wind regions. Results from a dedicated tool for the evaluation of SJ potential in windstorms, currently used operationally at the Met Office, are then discussed. All these results contribute to answering the key questions that stem from the impact of this storm, and the geographical distribution of it, namely: 'Was there a sting jet in Storm *Eunice*?' and 'Which of the strong-wind regions expected in a storm led to the observed wind gusts?' Indications coming from the results examined in this article will then be verified via a detailed model-based airstream analysis in the companion article (Volonté *et al*., 2023) of this two-part study.

Station observations of strong winds and gusts

The exceptionally strong winds and gusts caused by Storm *Eunice* are illustrated in Figure 2 using surface (10m) station observations at 1100 UTC 18 February. This time was chosen because it was when a record breaking 106kn (55ms^{-1}) gust was observed at the Needles Old Battery, off the west coast of the Isle of Wight (circled in Figure 2a). This gust exceeded the previous gust speed record for England recorded in 1979 (Kendon, 2022). While strong gusts are not unusual at the exposed location of the Needles Old Battery, a broad swath of gusts exceeding 50kn (26ms^{-1}) can be seen across southern England at this time. The corresponding mean surface wind speeds reached 55kn (28ms^{-1}) in the English Channel but were also strong over land, with almost all stations reporting speeds of at least 30kn (15ms^{-1}) (Figure 2b, which shows simplified station circles).

Winds at 1100 UTC in southwest England were generally westerly, changing to southwesterly in the southeast. The minimum central pressure for the stations shown is 976.4hPa, in north Wales, consistent with the Met Office analysis an hour later at 1200 UTC (not shown, but see earlier 0600 UTC analysis in Figure 1b), which indicated two low centres: one in the east Midlands region of 975hPa, associated with the strong winds, and a deeper centre of 971hPa over eastern Scotland. The two centres formed as the single low-pressure centre analysed at 1800 UTC on 17 February elongated northeastwards along the extending bent-back front (note that this front is marked as an occluded front in Figure 1b). The majority of England and Wales was overcast with 7 or 8 oktas of cloud reported (station circles mainly or entirely shaded); the exception to this is northeast England and East Anglia where the skies were much clearer, consistent with corresponding satellite imagery (see Figure 3d).

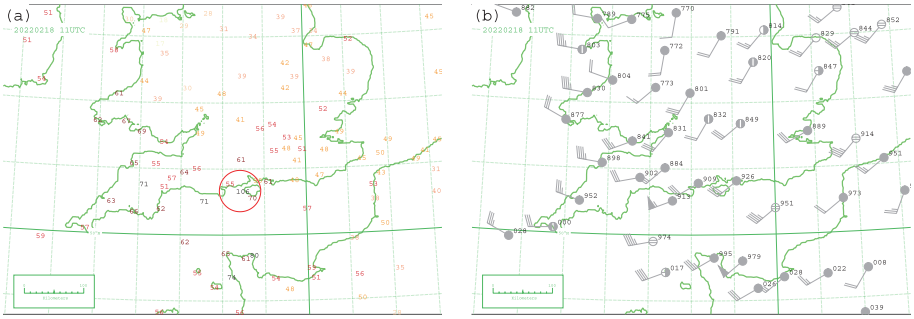

Figure 2. (a) Gust measurements (knots) at 1100 UTC coloured by value (stronger windspeeds are darker); the red circle indicates the location of the strongest wind gust. (b) Simplified station circles at 1100 UTC showing the total cloud amount (the filled circle), the wind (barbs in knots), and the mean sea-level pressure (in hPa) to the right of the circle, all in conventional notation (e.g. a plotted pressure value of 952 translates to 995.2hPa); the stations shown are required to have a minimum distance between them to limit over-plotting and hence not all available data are shown. All data are from the MetDB database, which holds data including surface and upper air observations and some satellite data (Met Office, 2008).

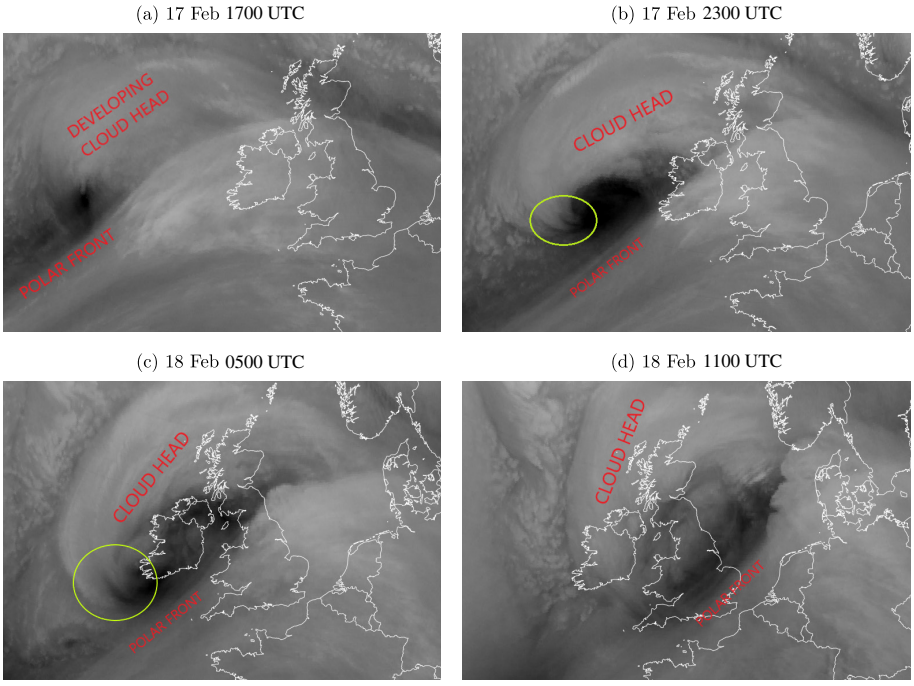

Figure 3. Satellite imagery from Meteosat SEVIRI water vapour channel (6.2μm) at the times indicated on top of the panels. Red text added by the authors highlights key cyclone features such as the cloud head (banded tip circled in yellow) and the polar front. (© EUMETSAT 2022.)

Satellite observations and indications of SJ activity

Satellite imagery displaying the structure of an intense cyclone can provide several indications of whether SJ activity is taking place, as illustrated in detail in Clark and Gray (2018). Such features can be found in the six-hourly spaced infrared satellite images covering the main stages of the evolution of Storm *Eunice* that are shown in Figure 3. In its initial stages of evolution, at 1700 UTC on 17 February, *Eunice* displayed a forming 'cloud head' (Bader *et al*., 1995), visible on the northern side of the polar front cloud band (Figure 3a). Six hours later, this cloud head, a distinctive trait of intense Shapiro–Keyser cyclones, is now fully formed and is associated with the formation of a bent-back front, separating the developing warm seclusion at the cyclone centre from colder air on its northern side (Figure 3b). At the same time, a 'dry wedge' (i.e., the dry slot) opens, separating the cloud head

from the polar front. The increasing distance between the tip of the cloud head and the polar front indicates that a frontal-fracture region was forming.

Near the tip of the cloud head, some 'finger-shaped filaments' are also visible in the imagery (see yellow circle in Figure 3b). These narrow clear bands in between cloud filaments, visible towards the tip of the cloud head, were first interpreted by Browning (2004) and Browning and Field (2004) as evidence of slantwise descent out of the cloud head and into the frontal-fracture region, and have been identified in most SJ cyclones since then. Hewson and Neu (2015) observe that the cloud filaments appear to dart forward while dissipating due to evaporation, giving the impression of a 'smoking gun', and that the gaps between them can extend forwards into holes in the low-level cloud deck. Clark and Gray (2018) point out that, although the available sample of cyclones is relatively small and there is no proven correspondence between banding and SJ activity, the circumstantial link between the two phenomena is quite strong. By 0500 UTC on 18 February, the cloud head had encircled the cyclone centre and the frontal-fracture region was beginning to close. Cloud-head banding is still evident, with one larger gap now opening at the cloud tip (yellow circle in Figure 3c). Finally, *Eunice* is shown in its mature stage in Figure 3d, with the bent-back front wrapped around the cyclone centre and the closing frontal-fracture region over South England. Figure 3d refers to 1100 UTC on 18 February, which is the same time as the wind observations shown in Figure 2, including the record-breaking gust at Needles Old Battery. At this time, the region between the dry slot and the cyclone centre was partially covered by clouds, with signs of local convection occurring. It is possible that some of those clouds were associated with strong winds in the frontal-fracture region impacting against low-level pre-existing air with different thermodynamic characteristics, in similar fashion to that shown in Browning and Field (2004) for the 'Great Storm', but further research would be needed to verify this.

To summarise, the various features described in this section are all typical of the evolution of an intense Shapiro–Keyser cyclone, compatible with SJ activity. In particular, a high likelihood of SJ activity is indicated by the presence of clear and sustained banding towards the tip of the cloud head.

Forecasts of strong winds and of potential SJ activity

Storm *Eunice* was forecast to become an intense cyclone several days in advance, with the first yellow Met Office wind warning for 18 February issued on 14 February, four days in advance of the storm crossing the UK and even two days before its genesis on 16 February. The warning was upgraded to amber on that date, with localised red warnings added from 17 February onwards (Met Office, 2022). These warnings are made based on the output of numerical forecasts produced by the Met Office and other agencies. Here we analyse output from three of the Met Office's forecast systems, all based on the Unified Model (MetUM), as an example of what is available to forecasters and as an attempt to understand the airstreams responsible for the strong winds associated with Storm *Eunice*.

First, we analyse results derived from the global 18-member ensemble MOGREPS-G (Bowler *et al*., 2008),[2] which has a 20-km grid spacing (N640, equal to 1280 longitude points and 960 latitude points) capable of representing synoptic-scale features and useful at estimating probabilities of event occurrence. While MOGREPS-G does not have the resolution to directly produce mesoscale features such as SJs, an indication of possible SJ activity in an already strong cyclone can be assessed, even days in advance, using a diagnostic tool described in Gray *et al*. (2021). This tool was implemented in 2019 as a forecaster's aid for the assessment of the severity of approaching cyclones. It is based on the assumption that while SJs might not be produced by a low-resolution model, precursor conditions leading to this phenomenon are still present in the forecast. The precursor that is diagnosed is the presence of a type of mesoscale instability called conditional symmetric instability (CSI), together with moisture available for the release of the instability, within the cyclone's cloud head. CSI exists when surfaces of saturated moist potential temperature are more tilted than surfaces of geostrophic absolute momentum, and if CSI is released, it leads to slantwise convection. This surface configuration also leads to saturated geostrophic potential vorticity being negative, and therefore, this is a necessary condition for CSI. Alternatively, CSI can be diagnosed via downdraught slantwise convective available potential energy (DSCAPE), which can be conceptualised as CAPE along surfaces of constant geostrophic absolute momentum; this is the CSI diagnostic used by the SJ precursor tool (see also text box in Gray *et al*., 2021). For readers familiar with (upright) CAPE, the precursor diagnostic is analogous to using the presence of large amounts of CAPE as an indicator that thunderstorms are likely to occur.

An example of the operational output available to forecasters from the SJ precursor tool is shown in Figure 4. The figures show the probability that a large, coherent region (more than 20 grid points within the cyclone above the DSCAPE threshold) of DSCAPE has developed with 200km of each grid point in the model domain. If the regions of DSCAPE in each ensemble member are large spatially then high probabilities will be signalled where they overlap within a broad region of lower probabilities. Conversely, if there are many regions of DSCAPE that are well-separated, then only the broad envelope of lower probabilities will be visible. Two different forecasts are shown: one initialised at 1200 UTC on 15 February and another on 17 February, with both being valid at 0000 UTC on 18 February. The output indicates a broad area where high values of DSCAPE are developing in the individual ensemble members. The broad yellow region indicates there is non-zero probability of an extended region of CSI developing (and therefore the potential for a SJ) for Storm *Eunice* even in the forecasts from 15 February (Figure 4a). The non-zero probability region is over Ireland and to the southwest of it in both panels in Figure 4, indicating consistency in storm evolution between the two forecasts. The probability shown is relatively small (up to 10% in localised spots) due to strong requirements on the location and areal extent of the region of large DSCAPE such that small difference between the location of the CSI in ensemble members can 'dilute' the signal. For example, the cyclone centres may be very close together in the ensemble, but the location of the cloud head may be significantly different due to variations in 3D storm structure introduced by the ensemble perturbations. However, the signal is present and is useful to forecasters assessing the potential severity of a storm. Thus, in the run up to *Eunice*, there was a sustained indication of CSI in the MetUM simulated cloud head, indicating a potential for SJ formation. Cyclone centres across the ensemble (indicated by coloured squares) are closer to each other between ensemble members in the 17 February forecast. This behaviour is expected as forecast uncertainty is reduced at shorter lead times.

We now discuss forecasts from the Met Office's global deterministic model that has an approximate 10-km grid spacing in the mid-latitudes (N1280, equal to 2560 longitude points and 1920 latitude points), which represents synoptic-scale features well and has a borderline capability to represent mesoscale features such as SJs (somewhat limited by vertical resolution). Forecasts produced with this model have a maximum lead time of six days. Four forecasts of wet-bulb potential temperature (θ_w) at 850hPa, wind speed at 850hPa and mean sea-level pressure all valid at 1200 UTC on 18 February are shown in Figure 5. These forecasts have

[2]Basic information on MOGREPS-G can also be accessed at https://www.metoffice.gov.uk/research/weather/ensemble-forecasting/mogreps.

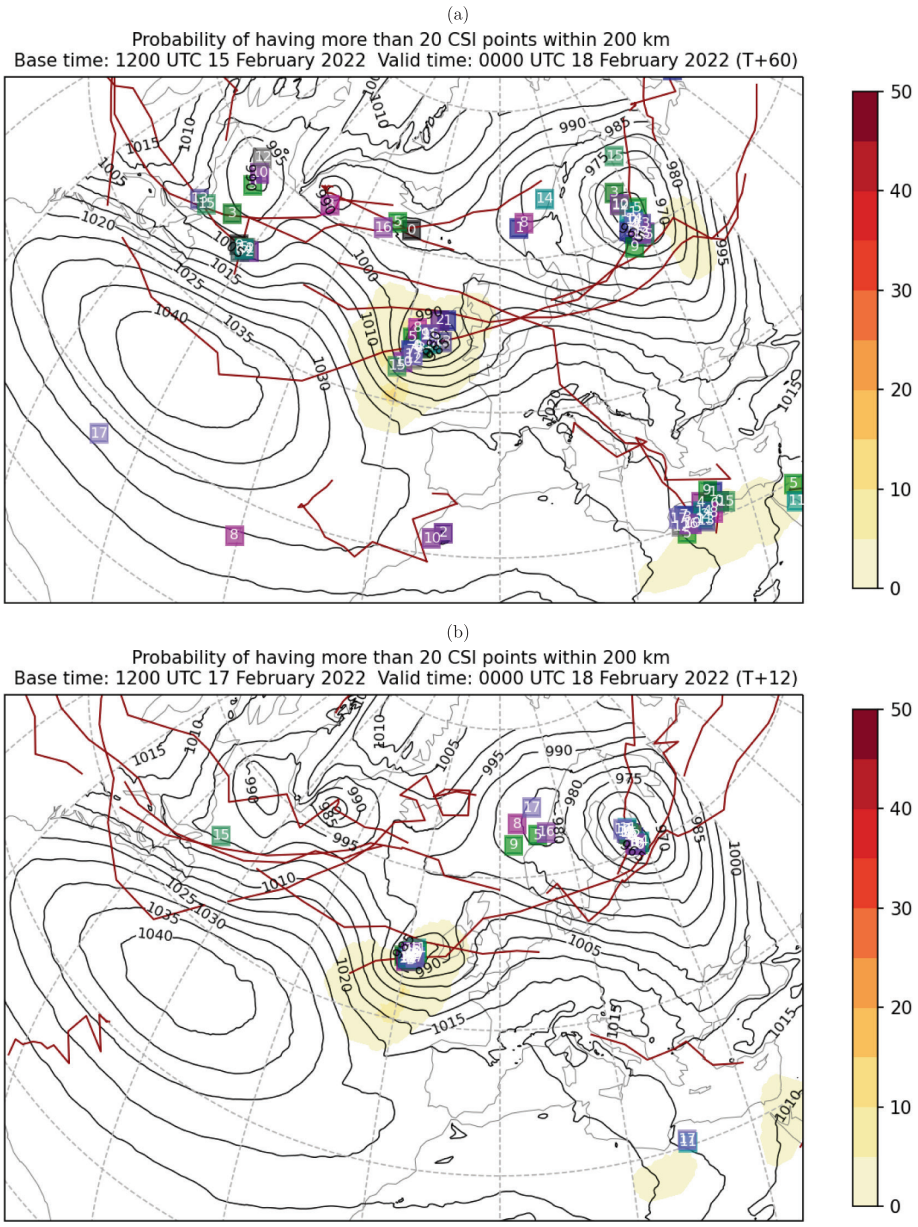

Figure 4. Ensemble-based probability of sting-jet precursor for greater than 20 CSI points (on a 0.5°×0.5° grid) within 200km (shaded), valid at 0000 UTC on 18 February, with data from the global operational UK Met Office forecasts initialised at (a) 1200 UTC on 15 February and (b) 1200 UTC on 17 February. The conditional symmetric instability (CSI) points are all within 1000km of a cyclone centre and constitute sets whose centroids are within 700km of a cyclone centre in the cloud head sector and with moisture available for the instability to be released. Overlain are the cyclone tracks of all the storms identified during the period (dark red lines) and the mean sea-level pressure (black contours every 5hPa) at the verification time from the control ensemble member. The squares along the tracks indicate the locations of the cyclone centres at the verification time colour-coded and numbered by ensemble member.

different lead times, decreasing from 120h (Figure 5a) to 0h (i.e. the analysis, Figure 5d). They all depict *Eunice* as a strong cyclone crossing the UK. Wind speed maxima exceeding 40ms^{-1} are present in all panels, with maxima exceeding 50ms^{-1} at 120 and 72h lead times. For lead times shorter than 72h there is a convergence of forecasts, with a mean sea-level pressure minimum located around the east-northeast English coast of ~970hPa. All those forecasts display the development of a warm seclusion at the cyclone centre with the storm moving towards a Shapiro–Keyser type, strong winds in the south quadrants of the cyclone and a localised area exceeding 40ms^{-1} between southeast England and the northeast France and Netherlands coasts. This maximum wind area lies in between the primary cold front to the east and the bent-back front tip to the west, in an area of slack θ_w gradients corresponding to the frontal-fracture region. This is the region where a SJ is expected to descend and, although this type of map does not distinguish between balanced cyclone winds and mesoscale jets such as the SJ, it is a first indication of strong winds being expected in that region.

MOGREPS-G and the global deterministic model show that the forecasts of Storm *Eunice* were very good on the synoptic scale, but at meso-β scales (20–200km), there was still significant uncertainty in the location and strength of winds and wind gusts. The third forecast product analysed here is the UK variable-resolution (UKV) model, which is a regional model covering the UK and surrounding ocean. It has a 4km grid spacing at the rim of the domain and a 1.5km grid spacing in the interior. Due to its high resolution, the UKV model is capable of directly reproducing features at the convective scale, providing a more realistic estimate of variables such as surface winds and wind gusts. Wind speed and gusts (at 10m) in the model analysis at 1200 UTC on 18 February and the forecast valid at the same time from the forecast cycle initialised at 0300 UTC 18 February are shown in Figure 6. Notice the correlation between these fields and 850-hPa wind speed (Figure 5d) that justifies the common use of the latter as a rough predictor of the former when a more sophisticated diagnostic is not available.

The model analysis in Figure 6a shows that the sustained wind speed drops much more than wind gusts from sea to land, decreasing from 24–26ms^{-1} over the English Channel to 16–18ms^{-1} over Southern England, while inland gusts still exceed 30ms^{-1} over land (with values between 35 and 40ms^{-1} over the sea). Maximum winds and gusts in Figure 6 are more to the east than in the observations in Figure 2, which are referred to 1h earlier. This is consistent with the storm gradually progressing eastward over the UK. A localised maximum over 40ms^{-1} is present in both forecast and analysis over the exposed coasts of East Sussex, while at 1100 UTC, a similar-sized maximum was present over the western and most exposed side of the Isle of Wight (not shown), collocated with the record-breaking gust observed at Needles Old Battery. The inland wind pattern in Figure 6a is also consistent with the observations illustrated in Figure 2 (taking into account the 1h difference and the eastward progression), both in terms of magnitude (as 30ms^{-1} is roughly equal to 58kn) and shape. Thus, strong 10m winds and gusts in the model analysis generally agree with those observed over southern England although there seems to be a slight overestimation over the Midlands. However, the earlier forecast (9h lead time, Figure 6b) overestimates winds and gusts, particularly over Wales and the Irish Sea but also over southeast England, where there are several local gust maxima exceeding 35ms^{-1} over land. This is also true for analyses and forecasts valid at 1100 UTC (not shown), with forecast winds dropping as lead time reduces.

These results show that even at short lead times, there is uncertainty in the forecasts,

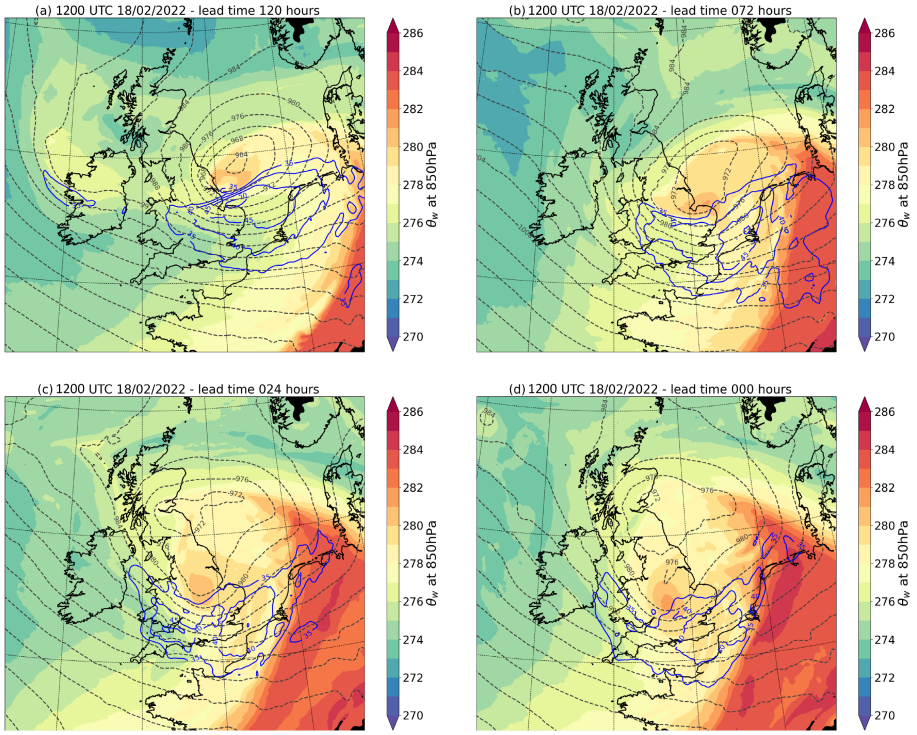

Figure 5. Wet-bulb potential temperature (shading, every 1K) at 850hPa, wind speed at 850hPa (blue contours, from 35ms^{-1} every 5ms^{-1}) and mean sea-level pressure (dashed grey contours, every 4hPa) valid at 1200 UTC on 18 February from UK Met Office global operational forecasts initialised at 1200 UTC on (a) 13 February, (b) 15 February, (c) 17 February and (d) analysis (see also the lead times stated in the panel titles).

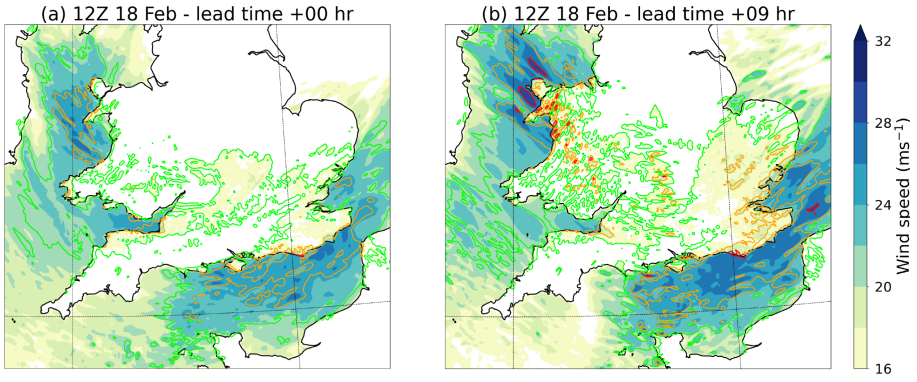

Figure 6. Wind speed (shading, ms^{-1}) and gusts (green contour for 30ms^{-1}, yellow for 35ms^{-1} and red for 40ms^{-1}) at 10m valid at 1200 UTC on 18 February from UK Met Office UK variable-resolution limited area analysis (a) and forecast initialised at 0300 UTC on 18 February (b). Note that Z time is equivalent to UTC.

leading to uncertainty on impacts. This uncertainty is caused in part by the complexity of dynamics of mesoscale airstreams that is crucial for near-surface extreme winds. These airstreams are the key focus of the companion article (Volonté *et al.*, 2023) in this two-part study, where we will tackle the question: 'Which structure of the storm is leading to the strong winds?'

Conclusions

Storm *Eunice* was an intense windstorm that affected the UK on 18 February 2022, triggering the first Met Office red warning for wind over southeast England since the NSWWS was set up in the wake of the Great Storm of 1987. *Eunice* produced record-breaking wind gusts over England and led to severe weather impacts, including fatalities, over the UK and Ireland.

Storm *Eunice* was forecast to become an intense cyclone several days in advance and displayed, both in observations and model forecasts, several specific features indicating the likely presence of SJ activity. These features include the evident banding at the tip of the bent-back cloud head present for several hours in satellite imagery.

The SJ precursor diagnostic tool, described in Gray *et al.* (2021) and available to Met Office operational forecasters, provided further indications of the potential for SJ activity in Storm *Eunice* up to three days in advance. However, uncertainty on the exact location and strength of near-surface peak winds was present in operational Met Office model forecasts even at lead times of just a few hours.

All the pieces of evidence just summarised indicate that SJ activity is likely to have occurred during the evolution of Storm *Eunice*. In particular, the presence of banding and holes at the tip of the cloud head over several hours point to a SJ being present for an extended period of time. However, the results contained in this article are not sufficient to conclusively determine whether the strong surface winds and gusts observed over southern England and Wales in the central hours of 18 February were associated with the descent of a SJ; additional and/or different airstreams cannot be ruled out. For this reason, and to provide more certainty on the identification of SJ activity, a detailed analysis of the main low-level airstreams present in Storm *Eunice* and of the underlying cloud-head dynamics was performed using Met Office operational model data. This analysis is presented in the second article (Volonté *et al.*, 2023) of this two-part study.

Acknowledgements

The work performed by Ambrogio Volonte was funded by the 2022 pump-priming fund of the Department of Meteorology, University of Reading. Oscar Martínez-Alvarado's contribution was supported by the UK Natural Environment Research Council as a member of the National Centre for Atmospheric Science. Duncan Ackerley is supported by the Joint BEIS/Defra Met Office Hadley Centre Climate Programme (GA01101) and facilitated the implementation of the DSCAPE diagnostic at the Met Office and access to the relevant datasets. The authors would also like to thank Dan Suri for leading the engagement process and subsequent development of the Met Office DSCAPE diagnostic and for providing helpful insight to an earlier version of this work. The implementation of the DSCAPE diagnostic at the Met Office was also supported by the UK Natural Environment Research Council through grant NE/S016384/1.

Author contributions

AV designed the study, performed the Eulerian analysis, and wrote a first draft of the article. SLG co-designed the study and performed the Lagrangian analysis, including the final schematic that AV then refined. Both authors discussed extensively the scope of the study and the results with PAC, OM-A and DA. All authors took part in

revising the document through the peer-review process.

Data availability

No new data were created in this study.

References

Bader MJ, **Forbes GS**, **Grant JR *et al***. 1995. *Images in Weather Forecasting. A Practical Guide for Interpreting Satellite and Radar Imagery*. Cambridge University Press: Cambridge.

Bowler NE, **Arribas A**, **Mylne KR *et al***. 2008. The MOGREPS short-range ensemble prediction system. *Q. J. R. Meteorol. Soc.* **134**(632): 703–722.

Browning KA. 2004. The sting at the end of the tail: damaging winds associated with extratropical cyclones. *Q. J. R. Meteorol. Soc.* **130**: 375–399.

Browning KA, **Field M**. 2004. Evidence from Meteosat imagery of the interaction of sting jets with the boundary layer. *Meteorol. Appl.* **135**: 663–680.

Burt SD, **Mansfield DA**. 1988. The great storm of 15–16 October 1987. *Weather* **43**(3): 90–110.

Clark PA, **Gray SL**. 2018. Sting jets in extratropical cyclones: a review. *Q. J. R. Meteorol. Soc.* **144**(713): 943–969.

Gray SL, **Martínez-Alvarado O**, **Ackerley D *et al***. 2021. Development of a prototype real-time sting-jet precursor tool for forecasters. *Weather* **76**(11): 369–373.

Hart NCG, **Gray SL**, **Clark PA**. 2017. Sting-jet windstorms over the North Atlantic: climatology and contribution to extreme wind risk. *J. Clim.* **30**(14): 5455–5471.

Hewson TD, **Neu U**. 2015. Cyclones, windstorms and the IMILAST project. *Tellus A* **67**(1): 27 128.

Kendon M. 2022. *Storms Dudley, Eunice and Franklin*, February 2022. Technical report, Met Office. https://www.metoffice.gov.uk/weather/learn-about/past-uk-weather-events. [accessed 10 March 2023].

Met Office. 2008a. *LAND SYNOP reports from land stations collected by the Met Office MetDB System*. NCAS British Atmospheric Data Centre. https://catalogue.ceda.ac.uk/uuid/9f80d42106ba708f92ada730ba321831 [accessed 30 March 2022].

Met Office. 2008b. *SHIP SYNOP reports from ship, buoy and fixed platform stations collected by the Met Office MetDB System*. NCAS British Atmospheric Data Centre. https://catalogue.ceda.ac.uk/uuid/65ca7898647cc3686492bcb8bb483a1c [accessed 30 March 2022].

Met Office. 2022. *Next Generation National Severe Weather Warning Service (NSWWS)*. Digital Library and Archive under Forecast Data & Analysis. https://digital.nmla.metoffice.gov.uk/ [accessed 10 March 2023].

Mühr B, **Eisenstein L**, **Pinto JG *et al***. 2022. CEDIM Forensic Disaster Analysis Group (FDA): Winter storm series: Ylenia, Zeynep, Antonia (int: Dudley, Eunice, Franklin) – February 2022 (NW & Central Europe). https://doi.org/10.5445/IR/1000143470.

Schultz DM, **Browning KA**. 2017. What is a sting jet? *Weather* **72**: 63–66.

Volonté A, **Gray SL**, **Clark PA *et al***. 2023. Strong surface winds in Storm *Eunice*. Part 2: airstream analysis. Weather **78**: https://doi.org/10.1002/wea.4401.

Correspondence to: A. Volonté
a.volonte@reading.ac.uk

doi: 10.1002/wea.4402